

# Switched Reluctance Generator for Low Speed Wind Turbines with Counter-Rotary Drive

Costica Nituca<sup>1\*</sup>, Dumitru Cuciureanu<sup>2</sup> and Gabriel Chiriac<sup>1</sup>

<sup>1</sup>Technical University "Gheorghe Asachi" Iasi, Faculty of Electrical Engineering, Bd. D. Mangeron, nr. 21- 23, Iasi - 700050 Romania; costica\_nituca@yahoo.com, gchiriac@tuiasi.ro  
<sup>2</sup>"Q" SRL Iasi, Stradela Sf. Andrei nr.13, Iasi, Romania; office@qsr.ro

## Abstract

**Background/Objectives:** To design a new type of switched reluctance generator for low speed wind turbines which operate at low speed wind. **Methods/Statistical Analysis:** Structure and operation principle of the proposed switched reluctance machine are described. The generator-wind turbine is a direct-drive one and has two mobile parts which can be droved by two wind turbines in counter-rotary motion. A test bench was achieved and two types of experiments were realized: first, with a part of the generator fixed and the other in rotary motion, and second with the both parts in motion. **Findings:** Using the counter-rotary motion it results an important increasing of the output voltage of the generator for the same speed. The generator can be used both for the turbines with horizontal or vertical axle, with some advantages for the vertical axes case, especially in urban area, where safe operation of vertical axis wind turbines requires low rotational speeds to reduce noise, mechanical vibrations and proximity hazards. **Applications/Improvements:** The proposed direct-drive generator is more efficient than the classical structure with gears and the simple rotary motion.

**Keywords:** Counter-Rotary Motion, Low Speed Wind, Switched Reluctance Generator, Wind Turbine

## 1. Introduction

In nowadays context of energy crisis and consuming of the resources, the optimal utilization of the regenerative energy is a priority. The wind energy is one of the opportunities to have more clean energy with fewer drawbacks. Estimated wind capacity by the year of 2020 is expected to increased to about 1 260 000 MW, which will be about of 12% of the world's electricity consumption<sup>1</sup>. There are three types of generator systems for wind turbines<sup>1</sup>. The first type is a fixed-speed wind turbine system using a multi-stage gearbox and a standard squirrel-cage induction generator. The second type (developed from 1990s) represents a variable speed wind turbine system with a multi-stage gearbox and a doubly fed induction generator, with a power electronic converter feeding the rotor winding. The third type is also a variable speed wind turbine, but with a direct-drive generator, usually a low-speed high-torque synchronous generator. A power electronic converter for the full-rated power is necessary

for the grid connection<sup>2,4</sup>. Usually, the conversion of the energy is realized by using the electric generators which are adapted to the parameters of the wind turbines. One solution is to use a step-up gear which increases the price, reduces the efficiency and needs maintenance. Heavy weight, large volume, noise, and vibrations are also significant drawbacks.

Another solution is to use a direct-drive Switched Reluctance Generator (SRG). This machine is robust, easy to construct, reliable, and it needs low maintenance. The use of power electronics and a good control will reduce some drawbacks as torque, current and voltage ripples and, as a consequence, the SRG has great developing potential in the area of wind power generation<sup>5-7</sup>. Distortion in main grid can disturb the protection equipments, being necessary supplementary tests and better protection to avoid interruption in power supply<sup>8,9</sup>. Some studies regard to produce the maximum output power at a given shaft speed for a SRG<sup>10</sup>. There is also interest in

\*Author for correspondence

harnessing wind power on-board of an electric vehicle using Switched Reluctance Generator (SRG) coupled to a wind turbine mounted on the vehicle<sup>11</sup>. Small-scale wind turbines are a solution for the energy consumption into the urban area and their modelling and analysis is a necessary step for their implementation<sup>12</sup>. Different controlling methods are used for the wind turbine applications, as neural network controller<sup>13</sup> or sliding mode control<sup>14</sup>.

Moreover, safe operation of the Vertical Axis Wind Turbines (VAWT) in restricted urban spaces requires low rotational speeds to reduce noise, mechanical vibrations and proximity hazards<sup>15</sup>. The VAWT are better adapted to be installed nearby the residential and urban areas because they have lower start-up speed and low noise level. These are also appropriate to be installed in areas with strong winds and, as an important advantage, the VAWT are indifferent to wind direction<sup>16</sup>.

In this paper a new type of switched reluctance generator for the variable low speed wind turbines with counter-rotary drive has been studied. It could be used for both vertical and horizontal axis wind turbines, in urban environments or in remote area without a grid connection.

## 2. The Wind Power

The kinetic energy of the air flow is estimated by using the energy flux density, which is the quantity of the energy which crosses, in a constant and uniform way, a unit surface normal to the wind direction in a unit of time. The specific power of an air flux is given by the relation (1)<sup>17-20</sup>, where the density of the air could be considered as constant, the wind turbines being usually less than 100 m high:

$$P = \frac{1}{2} \rho_{air} A v_{wind}^3 \tag{1}$$

Where  $\rho_{air} = 1.225 \text{ kg/m}^3$  is the air density,  $v_{wind}$  is the speed of the wind and  $A$  is the swept area.

For a surface of  $A = 1 \text{ m}^2$ , the variation of the specific power for the air flux is drawn in Figure 1, resulting significant values starting with a wind speed of about 8m/s. Therefore, the nominal speed of the large wind turbines is about 10÷15 m/s<sup>20</sup>. A duplication of the wind speed will give an increasing of 8 times for the power of the wind turbine, which is given by<sup>18,21,22</sup>:

$$P_{turbine} = \frac{1}{2} C_p \rho_{air} A v_{wind}^3 \tag{2}$$

where  $C_p$  is the power coefficient.

An efficient utilisation of the low speed wind can be obtained with two coaxial rotors with counter-rotary motion, which will give a double equivalent speed comparing with a single rotor system at the same dimensions. The solution is useful especially for low dimensions of the rotors (about two meters) and with speeds of about 500...600 rot/min<sup>17</sup>. Figure 2 shows the variation of the specific power of air flow at low speed of the wind. For the wind turbines with one rotor it has values between 0.61÷76.56 [W/m<sup>2</sup>] (curve 1), while, for the wind turbines with counter-rotary motion the power is double (curve 2), 1.22÷153.12 [W/m<sup>2</sup>]. These values are relatively low, but, with an optimization of the system, these powers could be used for low or medium power applications. The efficiency of the wind energy conversion is estimated by using a power coefficient  $C_p$ . The Betz model<sup>17</sup> is based on a tube of current with a constant area; for a wind turbine this area is the surface corresponding to the blades motion. In reality this surface is not constant. The maximum power  $P_{maxH}$  given at the rotor of a wind turbine with horizontal axle is<sup>17</sup>:

$$P_{maxH} = \frac{1}{2} \rho_{air} A v_{wind}^3 \frac{16}{27} \tag{3}$$

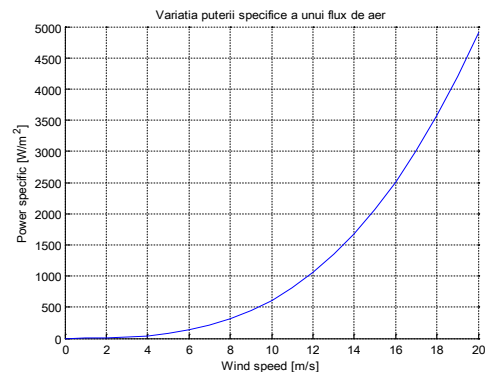


Figure 1. Specific power variation for the air flux.

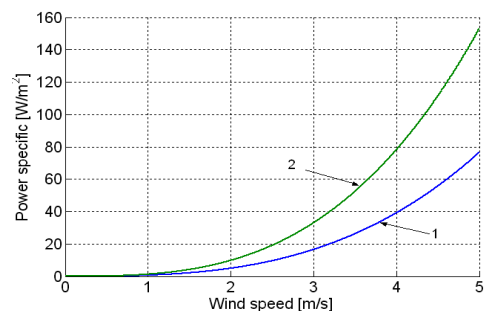


Figure 2. Specific power variation at low speed.

The power coefficient is:

$$C_p = \frac{P_{\max H}}{\rho_{\text{air}} A v_{\text{wind}}^3 / 2} = \frac{16}{27} = 0.59. \tag{4}$$

For a wind turbine with vertical axle the maximum power  $P_{\max V}$  and the power coefficient are<sup>17</sup>:

$$P_{\max V} = \frac{1}{2} \rho_{\text{air}} A v_{\text{wind}}^3 \frac{4\sqrt{5^3}}{25}, \tag{5}$$

$$C_p = \frac{4\sqrt{5^3}}{25} = 0.53. \tag{6}$$

The values resulted from using the global methods are higher than the real values. In the aerodynamic theory, there are proposed mathematical models which study the dynamic equilibrium of the forces, with more appropriate values on the real ones. An example for the wind turbine with vertical axle is by using the method of the tube currents with a single coefficient of influence. This method offers a calculus for different values of the solidity<sup>17</sup>,  $s = 0,2; 0,3; 0,4; 0,5; 0,6$  using the relations<sup>21</sup>:

$$s = NC / R_r, \tag{7}$$

$$\lambda = \omega R_r / v_{\text{wind}}, \tag{8}$$

$$\overline{F}_n^* = \frac{F_n^M}{\rho_{\text{air}} a C v_{\text{wind}}^2 / 2}, \tag{9}$$

$$C_p = \frac{P}{\rho_{\text{air}} a R v_{\text{wind}}^3}. \tag{10}$$

where:  $N$  -Number of the blades;  $R_r$  - Rotor radius;  $\omega$  -Angular speed of the rotor,  $F_n^M$  - Maximum normal force relative to a rotating blade;  $\overline{F}_n^*$  -Maximum normal force on the blade;  $a$  - influencing coefficient.

Considering the relations (7–10), in Figure 3 and Figure 4 are presented the force and the power coefficient. For this it was also considered the coefficient of lifting and the coefficient of resistance for the blade profile NACA 0012<sup>17</sup>. These theoretical methods are possible to apply while the constructive type of the wind turbine is corresponding to the model. Thus, for an optimal use of the low speed wind it is necessary to identify the type of turbine, the starting torque, the maximum power given by the wind and the optimum values of the speeds. For the wind turbines with vertical axle the best turbines are the ones with fixed blades and with oscillating blades<sup>17</sup>.

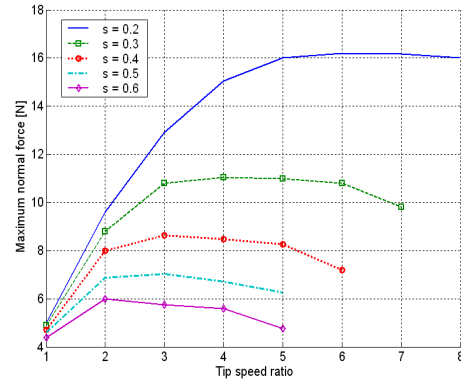


Figure 3. Maximum normal force on blade related to the tip speed ratio.

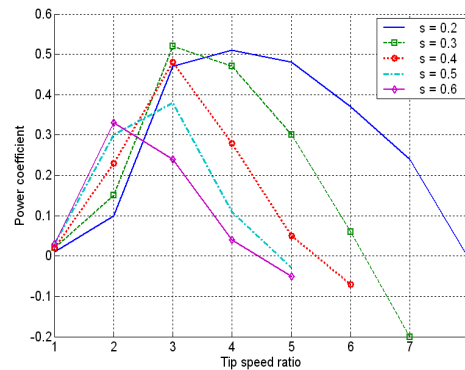


Figure 4. Power coefficient depending on the tip speed ratio.

In this situation, for the wind turbines with horizontal axle the best are the slow wind turbines (with many blades, which are adapted for low speed winds, at 1...3 m/s), at which the maximum efficiency is for a tip speed ratio of  $\lambda = 1$  and  $C_p = 0.3$ , that is for an energy intake of about 50% from the Betz limit. This value corresponds for an optimal rotation speed:

$$n = \frac{60 v_{\text{wind}}}{\pi D} \approx 19 \frac{v_{\text{wind}}}{D} \tag{11}$$

### 3. Structure and Operation Principle of the Proposed Switched Reluctance Machine

#### 3.1 Structure of the Proposed Switched Reluctance Machine

The construction of the proposed switched reluctance machine is presented in Figure 5. For this type of generator

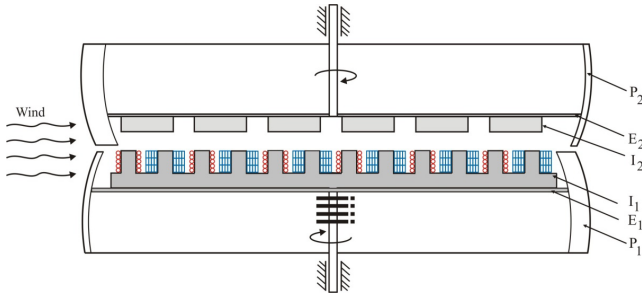


**Figure 5.** Schema of the proposal switched reluctance generator.

we will use the expressions “the function of inductor” and “the function of armature” and not the terms inductor and armature, because the both parts, the inductor and the armature, are in the same mechanical structure. This type of generator is proposed for operating at low speed because of some advantages as: simple construction, with the possibility to operate in counter-rotary regime; it is eliminated the kinematical chain because the turbine is directly connected to the axle of the turbine, so the energy loss are reduced; the generator is simple to adapt to the wind turbine operation both on constant or variable speed; there are no permanent magnets, so the costs are lower; the generator can operate in single-phase, three-phase or multi-phase construction.

The generator can be used both for the turbines with horizontal or vertical axle, with some advantages for the vertical axes case, especially in urban area, where safe operation of vertical axis wind turbines requires low rotational speeds to reduce noise, mechanical vibrations and proximity hazards. Also, they are well suited to such environments due to their inherent axisymmetric design<sup>15</sup>.

According to the Figure 5, the magnetic circuit with function of inductor and armature ( $I_1$ ), is built from sheet iron, fitted with teeth and notches which are uniformly distributed along the magnetic circuit, into a disc shape. Ahead of this circuit there is another disc magnetic circuit ( $I_2$ ), made up from a succession of elementary magnetic circuit with the same tooth pitch as the magnetic circuit ( $I_1$ ). These two parts, ( $I_1$ ) and ( $I_2$ ), can be droved in counter-rotary motion by two wind turbines ( $E_1$ ) and ( $E_2$ ), with vertical or horizontal axle. In the case of the horizontal axle, the counter-rotary motion is assured by a system of two counter-rotary co-axial turbines, while, for the vertical axle shown in Figure 5, the counter-rotary motion is assured by using two rotary turbines ( $E_1$ ) and ( $E_2$ ) with an appropriate orientation of the blades ( $P_1$ ) and ( $P_2$ ), so that, regardless the direction and the speed of the wind, the two turbines will have a counter-rotary motion.

This type of construction could have a small size (2 m diameter and 3 ÷ 4 m vertical axis) so they could be used on a special wind turbines in urban area on the rooftop of buildings, as discussed in<sup>23</sup>.

### 3.2 The Operation Phases of the Switched Reluctance Generator

The main operation phases of the switched reluctance generator are presented in Figure 6. On the odd teeth 1, 3, 5 are realized the D.C. operating windings. The odd teeth, 1, 5, 9, 13 (defined by the relation  $1 + 4n$ ,  $n = 1...30$ ), have operating windings which generate a positive excitation flux, while the odd teeth 3, 7, 11, 15,

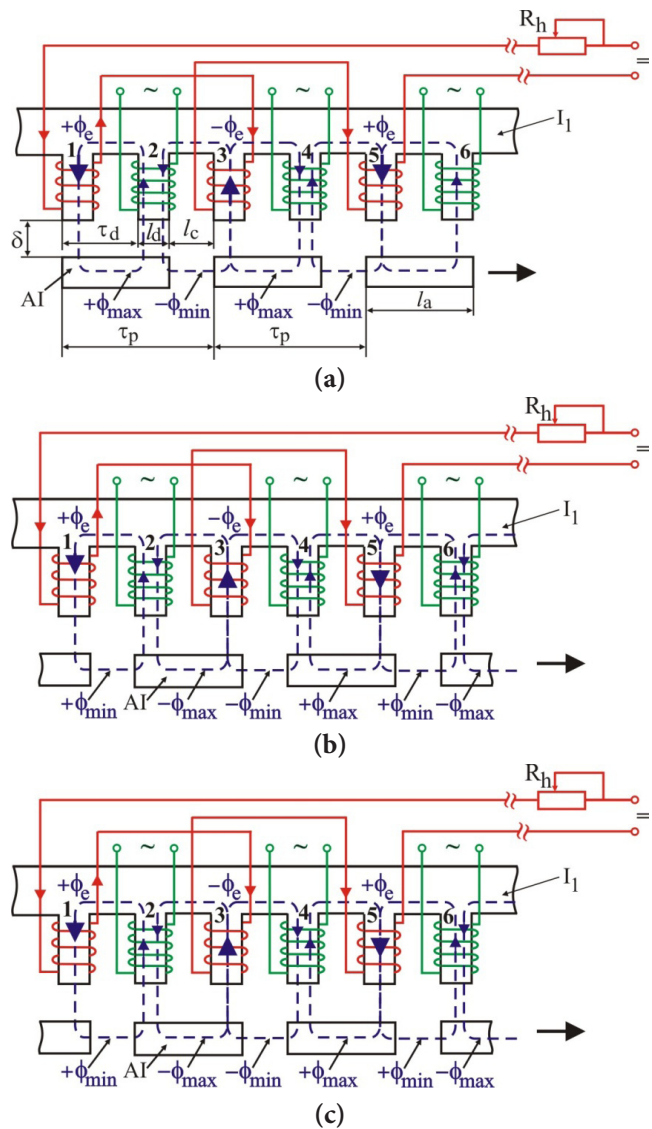


**Figure 6.** The main operation phases of the switched reluctance generator.

(defined by the relation  $3+4n$ ,  $n = 1...30$ ), have operating windings which generate a backward (negative) excitation flux, from the tooth to the yoke of the machine. All these odd teeth are actually field poles with small size and they have the function of an inductor. Between these teeth there are the even dental/teeth 2, 4, 6, 8 etc with windings that have function of armature windings. It is to observe that between the magnetic circuit with teeth and notch (at a distance  $\delta$  - air gap of the generator), there are some armatures for the inductor flux closing (denoted AI and arranged on a disk). The length of such an armature is  $l_a = \tau_d + l_d$ , where  $\tau_d$  is the tooth pitch, and  $l_d$  is the width of a tooth. In Figure 6.a. the closing armature AI is exactly in front of two teeth, 1 and 2, and of a notch. The positive flux ( $+\Phi_c$ ) created by the pole no. 1 closes by the tooth 1, air gap, the armature AI, air gap, the tooth no. 2 with the role of armature, by joke and again the tooth no. 1. The total air gap is minimum, that is  $2\delta$ , and the flux will be maximum, because the reluctance is minimum.

In Figure 6.b. the closing armature AI is moved a half of a tooth pitch, the edges of the armature being in front of the sideways of the teeth 1 and 3, and its middle being in front of the tooth no. 2, which has a role of armature. Along of a flux line it will be two air gaps and a quarter of circle at the right edge of the armature AI. The flux in tooth no. 1 is decreasing at ( $+\Phi_{min}$ ) and will cross the tooth no. 2. At the same time, the pole on the tooth no. 3 will also generate a minimum flux ( $-\Phi_{min}$ ), but in opposite direction ( $-\Phi_c$ ), which will cross the tooth no. 2 in opposite direction and will cancel the effect of the flux ( $+\Phi_{min}$ ). Thus, in this position of the armature, in the tooth no.2 the total flux will be zero. Continuing its movement, the armature AI will be in front of the teeth 2 and 3. Through the tooth no. 3 will cross a maximum flux, but with an opposite sign,  $-\Phi_{max}$  and a positive flux  $+\Phi_{max}$ , which will also cross through the tooth no.2. As a consequence, it will be crossed by the difference between the two fluxes ( $-\Phi_{max} + \Phi_{min}$ ). During a variation cycle, the armature coil on the tooth no. 2 will be crossed alternatively by the flux variation given by ( $+\Phi_{max} - \Phi_{min} > 0$ ) and ( $-\Phi_{max} + \Phi_{min} < 0$ ). To estimate the variation space of this flux at the new type of generator, let us consider the space which has to be crossed in a complete variation period  $S_{pvc}$ . For this it can be written the relations:

$$\begin{aligned} S_{pvc} &= 2\tau_p, \text{ but } \tau_p = 2\tau_d, \text{ and it results,} \\ S_{pvc} &= 2 \cdot 2\tau_d = 4\tau_d, \end{aligned} \quad (12)$$

where  $\tau_p$  is pole pitch.

The proposal generator has a large number of poles, both as inductors and as armatures but of small size. This allows to put in series many induced windings and so the resulted voltage will have significant values even for low speed variation of the inductor flux. The efficiency of the machine depends on the ratio between the maximum and minimum reluctance.

## 4. Experimental Data

Two types of experiments were realised. First experiment was realized with a part of the generator ( $I_1$ ) fixed and the other part ( $I_2$ ) in rotary motion, droved by an electric motor M2 (the K2 switch is closed) shown in Figure 7. A second experiment was realized with the both parts of the generator in motion (both K1 and K2 are closed). The two motors are permanent magnet motors (24 V, 120 W, 150 rpm) and they drive the ( $I_1$ ) and ( $I_2$ ) in counter-rotary motion, which simulates the rotation of the two wind turbines ( $E_1$ ) and ( $E_2$ ).

The air gap is of 4 mm and the diameter of the generator is 1 m. For both experiments the generator was droved with speeds corresponding to the wind speed of 0.5...4 m/s, respectively 9.5...76 rot/min. In order to start from a low speed, the inductor windings are supplied from a D.C. source with an excitation voltage of  $U_{exc} = 10.5 \div 29.4$  V, and an excitation current of  $I_{exc} = 0.5 \div 1.5$  A. The generator will deliver power to a resistive circuit with a value of  $R_s = 2\Omega$ . Figure 8.a presents the load diagram of the generator  $U_{gen} = f(I_{exc})$  for the first experiment, with ( $I_1$ ) fixed and ( $I_2$ ) in rotary motion for speeds between 9.5 rot/min to 76 rot/min. It is noted that as the excitation current increases between  $I_{exc} = 0.5 \div 1.5$  A, the voltage

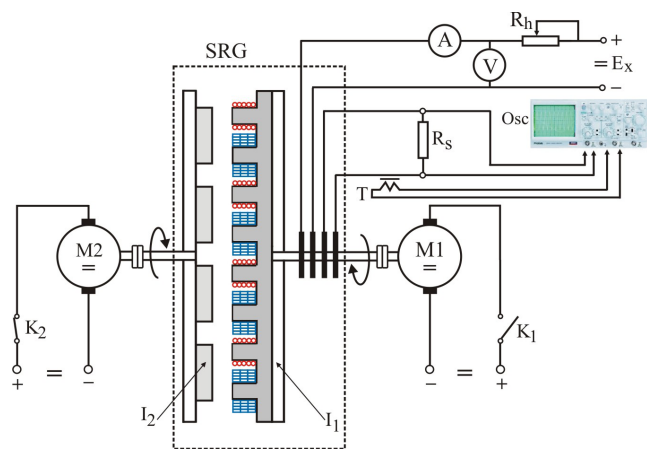
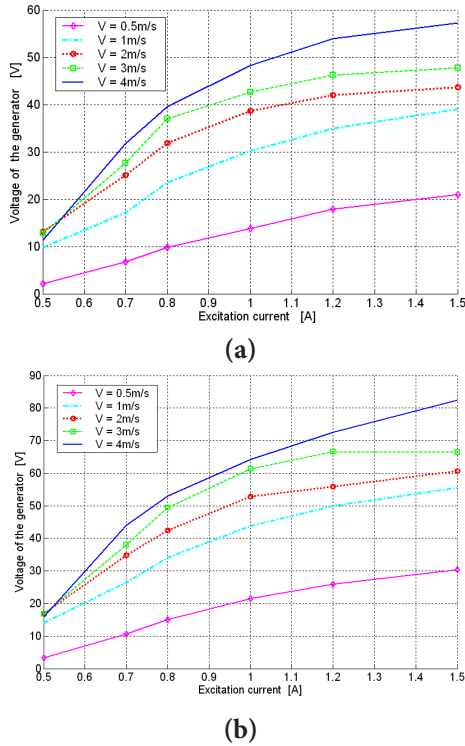


Figure 7. The schema of the experimental bench.



**Figure 8.** (a)  $U_{gen} = f(I_{exc})$  characteristics for the simple rotary motion (b)  $U_{gen} = f(I_{exc})$  characteristics for the counter-rotary motion.

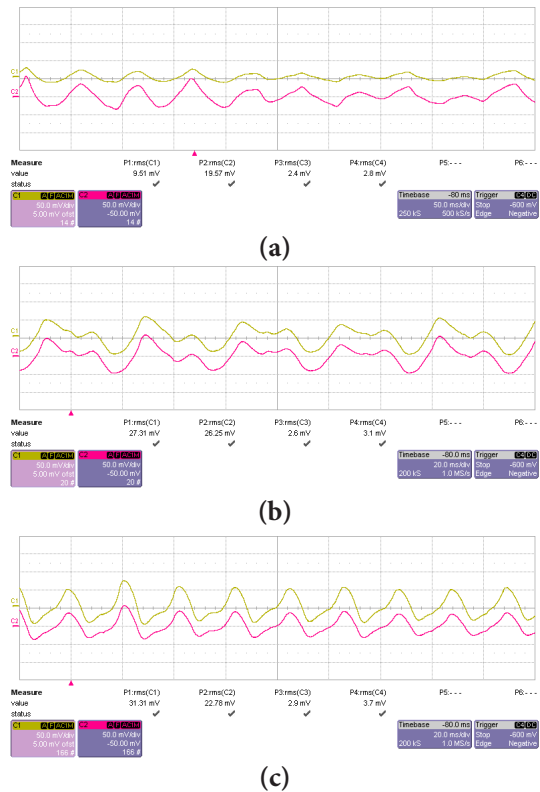
at the terminals of the generator is also increasing to a maximum value corresponding to the saturation process of the magnetic circuit. The voltage is increasing also with the speed, having a minimum value of  $U_{gen} = 2.12V$  for an initial current of  $I_{exc} = 0.5 A$  and for a speed of  $0.5 m/s$  (9.5 rot/min) and reaching a maximum value of  $U_{gen} = 57.26 V$  for  $I_{exc} = 1.5 A$  and for a speed of  $4 m/s$  (76 rot/min). For an excitation current of  $0.5 A$  and for the others speeds (from  $1 m/s$  to  $4 m/s$ ) the voltage has narrow values of about  $9.78...13.2 V$ .

Figure 8.b presents the load diagram of the generator  $U_{gen} = f(I_{exc})$  for the second experiment, with  $(I_1)$  fixed and  $(I_2)$  in counter-rotary motion for the same speeds, between 9.5 rot/min to 76 rot/min. It is noted that for  $I_{exc} = 1.5A$ , the voltages at the terminals of the generator are higher than in the first experiment (considering the same speeds):

- for  $v_{wind} = 0.5 m/s, n = 9.5rot/min, I_{exc} = 1.5 A$ , it results  $U_{genI} = 20.91 V, U_{genII} = 30.31 V$ , so  $U_{genI} < U_{genII}$  ;
- for  $v_{wind} = 1 m/s, n = 19 rot/min, I_{exc} = 1.5 A$ , it results  $U_{genI} = 39.08V, U_{genII} = 55.49V$ , so  $U_{genI} < U_{genII}$  ;
- for  $v_{wind} = 2 m/s, n = 38 rot/min, I_{exc} = 1.5 A$ , it results  $U_{genI} = 43.6 V, U_{genII} = 60.6 V$ , so  $U_{genI} < U_{genII}$  ;

- for  $v_{wind} = 3 m/s, n = 57 rot/min, I_{exc} = 1.5 A$ , it results  $U_{genI} = 47.8, U_{genII} = 66.4V$ , so  $U_{genI} < U_{genII}$  ;
- for  $v_{wind} = 4 m/s, n = 76 rot/min, I_{exc} = 1.5 A$ , it results  $U_{genI} = 57.26V, U_{genII} = 82.45V$ , so  $U_{genI} < U_{genII}$  ;
- $U_{genI}$  is the voltage at the terminals of the generator for the first experiment;
- $U_{genII}$  is the voltage at the terminals of the generator for the second experiment.

The experimental tests have been performed using a digital oscilloscope type LeCroy Wave Surf 400 with four channels. On the Channel 1 was measured the current of the generator on a resistive load with  $R_s = 2\Omega$ , by a Hall transducer LA55-P (with a ratio of 50A/50 mA). The waveform has been recorded with a measurement resistance of  $100\Omega$ , resulting a new ratio of 50A/5V. The output voltage at the terminals of the generator was measured by a voltage Hall transducer with a ratio of  $k = 500$  (on Channel 2). Figure 9 presents four oscillograms with waveforms for voltage and current at different speeds of the induced circuit ( $I_2$ ). For these tests the voltage and the current had the values  $U_{exc} = 10.5V, I_{exc} = 0.5A$ . Figure 9.a. presents the



**Figure 9.** (a) Waveforms for a speed of 1 m/s. (b) Waveforms for a speed of 2 m/s. (c) Waveforms for a speed of 4 m/s.

waveforms for a speed of 1 m/s (19 rot/min for  $I_2$ ). It is to notice a small value of the current  $I_g = 0.15A$  for a voltage of  $U_{gen} = 9.78V$ . The waveforms are not sinusoidal and have important harmonics.

In Figure 9.b. the value of the current is increasing to 0.24A and the voltage to 13.12V. An important aspect is the fact that the waveform of the current is in phase with the waveform of the voltage because of the resistive load. The speed of the induced circuit ( $I_2$ ) is of 2 m/s (28 rot/min). The last oscillogram (Figure 9.c.) has been recorded for a speed of 4 m/s (76 rot/min). The current increases to 0.33A and the voltage decreases from 12.7V to 11.39V. As above, both the output current and the output voltage of the generator are in phase.

## 5. Conclusions

A new type of Switched Reluctance Generator (SRG) for the low speed wind turbines with vertical or horizontal axle is presented. The solution generator-wind turbine is a direct-drive one and has two mobile parts which can be droved by two wind turbines in counter-rotary motion by the appropriate orientation of the blades. A test bench was achieved, with the two mobile parts driven by two electric motors with variable speed. Experimental data has been obtained and analyzed for two situations: first, when the mobile part ( $I_1$ ) is stationary-fixed and the mobile part ( $I_2$ ) is free to rotate and second, when both elements ( $I_1$ ) and ( $I_2$ ) are free to rotate in counter-rotary motion. Using the counter-rotary motion it results an important increasing of the output voltage of the generator for the same speed. Thus, the proposed direct-drive generator is more efficient than the classical structure with gears and the simple rotary motion.

### Nomenclature

$P$	- The specific power of the air flux;
$P_{turbine}$	- The power of the wind turbine;
$\rho_{air}$	- The air density;
$A$	- Swept area of the blades;
$v_{wind}$	- The speed of the wind;
$C_p$	- Power coefficient; the fraction of the wind power that is captured by wind turbine blades;
$s$	- Turbine solidity;
$\lambda$	- Tip speed ratio;
$N$	- Number of the blades;
$R_r$	- The radius of the rotor;
$\omega$	- The angular speed of the turbine;
$F_n^M$	- The maximum normal force on the blade;

$F_n^M$	- The maximum relative normal force on the blade for a rotation;
$\delta$	- The air gap of the generator;
$l_a$	- The length of a simple magnetic circuit for flux closing;
$\tau_d$	- The tooth pitch;
$\tau_p$	- The pole pitch;
$l_d$	- The width of a tooth;
$l_c$	- The width of a notch;
$S_{pvc}$	- The space of complete variation of the induced flux;
$U$	- The terminal voltage;
$I$	- The phase current;
$R$	- The phase resistance;
$\Phi$	- The flux linkage;
$P_{gen}$	- The power of the generator;
$u_{exc}$	- Voltage supply on the inductive windings;
$i_{exc}$	- The current in the inductive windings;
$u_{gen}$	- The output voltage of the generator;
$i_{gen}$	- The current on the terminals of the generator;

## 6. References

- Li H, Chen Z. Overview of different wind generator systems and their comparisons. IET Renewable Power Generation. 2008; 2(2):123–38.
- Polinder H, Bang DE, Li H, Chen Z. Concept report on generator topologies, mechanical and electromagnetic optimization. Project up Wind. 2007.
- Zuher A, Mehrdad K. An analytical literature review of stand-alone wind energy conversion systems from generator viewpoint. Renewable and Sustainable Energy Reviews. 2013; 28:597–15.
- Polinder H, De Haan SWH, Dubois MR, Slootweg JG. Basic operation principles and electrical conversion systems of wind turbines. 4<sup>th</sup> Nordic Workshop on Power and Electronics and Drives; 2005; 15(4):43–50.
- Darie E, Cepisca C. The use of Switched Reluctance Generator in wind energy applications. In: Hammons TJ, editors. 13<sup>th</sup> Renewable Energy, in Technology; 2007. p. 448–62.
- Arifin A, Al-Bahadly IH, Mukhopadhyay SC. State of the Art of Switched Reluctance Generator. Energy and Power Engineering. 2012; 4:447–58.
- Arifin A, Al-Bahadly IH. Switched reluctance generator for variable speed wind energy applications. Smart Grid and Renewable Energy. 2011; 2(1):227–36.
- Plesca A, Scintee A. Testing of power electrical apparatus using modular high current source. IREE. 2010; 5(3):1218–24.

9. Plesca A. Busbar temperature monitoring and correlation with protection electrical apparatus. *IREE*. 2011; 6(5):2659–65.
10. Choi DW, Byun SI, Cho YH. A study on the maximum power control method of switched reluctance generator for wind turbine. *IEEE Transactions on Magnetics*. 2014; 50(1).
11. Bao YJ, Cheng KWE, Cheung NC, Ho SL. Experimental examination on a new switched reluctance wind power generator system for electric vehicles. *IET Power Electronics*. 2012; 5(8):1262–9.
12. Ajao KR, Mahamood MR, Iyanda MO. Interface for modeling the power output of a small wind turbine. *Indian Journal of Science and Technology*. 2009 May; 2(5).
13. Rajaji L, Kumar C. neural network controller based induction generator for wind turbine applications. *Indian Journal of Science and Technology*. 2009 Feb; 2(2).
14. Menon Parvathy V, Gnanambigai M. Stability analysis of the variable speed wind turbine using sliding mode control. *Indian Journal of Science and Technology*. 2015 Apr; 8(S7).
15. Yen J, Ahmed N. Improving safety and performance of small-scale vertical axis wind turbines. *Procedia Engineering*. 2012; 49:99–106.
16. Messineo Av, Culotta S. Evaluating the performances of small wind turbines: A case study in the South of Italy. *Energy Procedia*. 2012; 16:137–45.
17. Ilie V, Almasi L, Nedelcu S. *Utilizarea energiei vantului*. Tehnica, Bucuresti. 1984.
18. Patel MR. *Wind and Solar Power Systems*. New York: CRC Press; 1999.
19. Bostan I, Dulgheru V, Sobor Iv, Bostan V. *Sisteme de conversie a energiilor regenerabile: Eoliana, solara, hidraulica*. Tehnica-Info, Chisinau. 2007.
20. Martinez J. *Modelling and Control of Wind Turbines*. London, UK: Imperial College; 2007.
21. Barros TA, Dos S, Filho AJS, Filho ER. Direct Power Control for Switched Reluctance Generator. In: Muyeem M, (editor). *Wind Energy, Modeling and Control Aspects of Wind Power Systems*. USA: Intech; 2013.
22. Nassereddine M, Rizk J, Nagrial M. Switched reluctance generator for wind power applications. *World Academy of Science, Engineering and Technology*. 2008; 2(5):583–7.
23. Fiedler AJ, Tullis S. Blade offset and pitch effects on a high solidity vertical axis wind turbine. *Wind Engineering*. 2009; 33(3):237–46.